Lawrence Berkeley National Laboratory
Recent Work

Title
Method of Measuring Nighttime U-Values Using the Mobile Window Thermal Test Facility

Permalink
https://escholarship.org/uc/item/19d1d00c

Author
Klems, J.H.

Publication Date
1992-04-01

eScholarship.org Powered by the California Digital Library
University of California

LBL-30032
UC-350

Lawrence Berkeley Laboratory

UNIVERSITY OF CALIFORNIA

ENERGY & ENVIRONMENT DIVISION

Presented at the ASHRAE 1992 Annual Meeting,
Baltimore, MD, June 27–July 1, 1992,
and to be published in the Proceedings

Method of Measuring Nighttime U-Values Using the Mobile Window Thermal Test (MoWiTT) Facility

J.H. Klems

April 1992

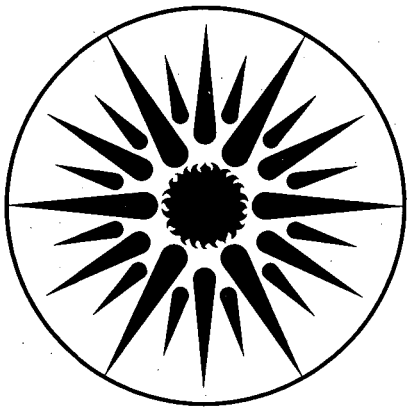

ENERGY & ENVIRONMENT DIVISION

Prepared for the U.S. Department of Energy under Contract Number DE-AC03-76SF00098

| LOAN COPY |
|Circulates |
|for 4 weeks| Bldg. 50 Library.
Copy 2
LBL-30032

DISCLAIMER

This document was prepared as an account of work sponsored by the United States Government. While this document is believed to contain correct information, neither the United States Government nor any agency thereof, nor the Regents of the University of California, nor any of their employees, makes any warranty, express or implied, or assumes any legal responsibility for the accuracy, completeness, or usefulness of any information, apparatus, product, or process disclosed, or represents that its use would not infringe privately owned rights. Reference herein to any specific commercial product, process, or service by its trade name, trademark, manufacturer, or otherwise, does not necessarily constitute or imply its endorsement, recommendation, or favoring by the United States Government or any agency thereof, or the Regents of the University of California. The views and opinions of authors expressed herein do not necessarily state or reflect those of the United States Government or any agency thereof or the Regents of the University of California.

LBL-30032
Mo-289

Presented at the ASHRAE Annual Meeting in Baltimore, MD, in June 1992, and to be published in *ASHRAE Transactions*, Vol. 98, Part 2.

Method of Measuring Nighttime U-Values Using the Mobile Window Thermal Test (MoWiTT) Facility

J.H. Klems
Windows and Daylighting Group
Energy and Environment Division
Lawrence Berkeley Laboratory
1 Cyclotron Road
Berkeley, California 94720

April 1992

This work was supported by the Assistant Secretary for Conservation and Renewable Energy, Office of Building Technologies, Building Systems and Materials Division of the U.S. Department of Energy under Contract No. DE-AC03-76SF00098

Method of Measuring Nighttime U-Values Using the Mobile Window Thermal Test (MoWiTT) Facility

ABSTRACT

Although primarily designed for studying the dynamic net energy flows through fenestration systems over the full diurnal cycle, the Mobile Window Thermal Test (MoWiTT) Facility is also frequently used to measure nighttime U-values. These measurements have the advantage of incorporating the exterior film coefficient resulting from the true ambient conditions at a particular time and location, rather than relying on a laboratory simulation of some assumed average or extreme condition. On the other hand, the MoWiTT is a much more complicated facility than a laboratory hot box, and the number of potential error sources is correspondingly larger. The method of deriving the nighttime U-value from directly measured data and the effect of random and systematic errors are discussed.

INTRODUCTION

Fenestration nighttime U-values are typically measured in a laboratory hot box arranged to simulate some prototypical operating condition, the most commonly-used of which is the "ASHRAE standard" condition of 70°F interior temperature, 0°F exterior temperature, and an exterior film coefficient equivalent to a 15 mph wind blowing directly on the sample. Laboratory U-value measurements are then taken as indicators of the relative wintertime performance of different fenestrations. Doing this requires making two assumptions: (1) that thermal heat loss is the principal determinant of relative winter performance and (2) that the U-values measured for different fenestrations under laboratory conditions faithfully represent the direction and magnitude of differences in the thermal heat loss of the fenestrations under conditions of actual application. Assumption (2), in other words, concerns whether the laboratory conditions are correctly representative of actual performance. There has historically been considerable controversy over this issue as it concerns the choice of test conditions or the particular implementation of the conditions in the laboratory. It has also been shown (Berman and Silverstein 1975) that, because of the importance of wintertime solar heat gain, assumption (1) is by no means automatically true and that one must exercise care in using U-values to predict differences in energy use. Nevertheless, U-values have remained the principal yardstick for comparing wintertime fenestration performance.

In the Mobile Window Thermal Test (MoWiTT) Facility (Klems et al. 1982), shown in Figure 1, a different basic approach is used. The measure of relative performance between two fenestrations is taken to be the dynamic net energy flowing through each of them under ambient conditions, which during the day includes direct and diffuse solar irradiation. For this reason, the MoWiTT was designed to utilize a roomlike interior environment and ambient weather conditions, to be capable of measuring two fenestrations simultaneously under the same conditions, and to measure net heat flows over relatively short time periods under non-steady-state conditions. At nighttime, however, the net energy flow can readily be converted into a U-value measurement, and the long-term average of these measurements must correspond to a steady-state measurement (at some set of temperatures and wind speed). Thus, the MoWiTT is capable of measuring the U-value under field conditions, and comparison with laboratory measurements (or calculations under

standard assumptions) may shed some light on the question of the validity of Assumption (1). In this paper we discuss how the measurement and conversion to U-value was carried out.

In every case where a fenestration U-value measurement is compared with another value (which might be either another measurement under the same conditions, a calculation, a measurement of the same fenestration under different conditions, or a measurement or calculation for a different fenestration), the question inevitably arises whether the difference obtained is significant, i.e., whether it arises from errors in the measurement process or from true differences in the underlying physical situation. To answer this question requires a quantitative knowledge of the potential error sources in the measurement and its interpretation; accordingly, a substantial part of this paper is spent elucidating these error sources for the MoWiTT.

DETERMINATION OF U-VALUES

The basic measurement produced by the MoWiTT is a measurement of the net heat flow, $W(t_n)$, where $t_n = t_0 + n\,\tau$ is the time of the n^{th} data recording, and $W(t_n)$ is an average over the period t_{n-1} to t_n. The data recording period τ may be varied but is generally kept at 10 minutes. W is determined calorimetrically as the sum of energy addition and subtraction rates from a variety of sources, to be enumerated below. The basic measurements composing W are sampled approximately every five seconds, so that each recorded value is an average over approximately 120 measurements. Similarly sampled, averaged, and recorded are an array of temperature sensors used to construct $T_I(t_n)$, the mean calorimeter air temperature; $T_O(t_n)$, the exterior air temperature; and a large number of auxiliary quantities, such as solar intensity, wind speed and direction, and temperatures at various locations, that aid with interpretation of the measured data. T_I and W are, of course, separately measured and recorded for each of the two calorimeter chambers.

W actually represents the total power flowing through the area not covered by the large-area heat flow sensors mounted on the interior surfaces of the calorimeters, as shown in Figure 2. Accordingly, a mask or flanking heat loss correction is necessary to obtain the total power flowing through the test sample. It sometimes happens that T_I varies somewhat with time during the measurement period (this is usually due to control system problems). In this case, a correction for heat storage in the calorimeter chamber is also necessary. Both of these corrections are discussed in detail below. The corrected net heat flow per unit time through the sample is thus

$$W_S(t_n) = W(t_n) - M[T_O(t_n) - T_I(t_n)] - C\frac{dT_I}{dt}(t_n). \qquad (1)$$

By convention, W is defined as positive for heat flows into the chamber, hence the ordering of the temperatures in the mask correction, M.

The U-value averaged over the n^{th} sampling interval is then calculated as

$$U(t_n) = \frac{W_S(t_n)}{A_T[T_O(t_n) - T_I(t_n)]}, \qquad (2)$$

where A_T is the area of the test sample. In order to avoid certain known biases in the measurement, data for U-values are taken only between midnight PST and sunrise, where sunrise is defined to occur when the pyranometer measuring incident solar energy at the plane of the window registers a

positive reading. (This typically occurs before the sun appears above the horizon, due to diffuse scattering in the atmosphere.) Data over many sampling intervals (typically extending over approximately one week) are averaged to obtain the steady-state U-value. Measurements of associated variables, such as T_I, T_O and wind speed, are averaged over the same time period and with the same selection criteria to determine the average conditions to which the measured steady-state U-value applies.

EXPERIMENTAL ERRORS AND BIAS

Although the equation (2) for measured U-value appears simple, in the MoWiTT the measured net heat flow W is a quantity derived from a somewhat complex measurement process. Before discussing the experimental errors arising from that measurement process, it is useful to make a few definitions and distinctions.

As discussed in Appendix A, which reviews the theory underlying our error-estimating procedure, any experiment may be viewed as a series of measurements used to determine the most probable values of a set of parameters $\{a_k^*\}$ appearing in a theory that describes the measurement apparatus. These parameters, in general, include both the physical variables resulting from the measurement (for example, the temperature computed from the measured resistance of an RTD) and parameters characterizing the apparatus (for example, the constants appearing in the equation describing behavior of the RTD). The experimental result (here denoted U) is then calculated as a function of those parameters:

$$U^* = f(a_j^*). \tag{3}$$

It is useful to divide the parameters into the physical outputs of the measurement (e.g., temperature), which we denote p_k, and the apparatus characteristics, which we denote c_ℓ (j,k, and ℓ are identifying indices: j=1,...,P; k=1,...,K; ℓ=1,...,L; where P=K+L). As indicated in the example of the RTD in Appendix A, a measurement may in reality consist of two (or more) separate experiments, which we denote here by the subscripts M and C. In experiment C (the calibration experiment), a series of N_C measurements of a set of variables (z_1, ..., z_C) is used to determine all of the parameters in the theory and in particular the values of $\{c_\ell\}$, which characterize the apparatus. In experiment M, the measurement proper, the values of the $\{c_\ell\}$ are held constant and N measurements of a set of variables (x_1, ...,x_M) are used to determine the physical outputs $\{p_k\}$. The result of the experiment is then

$$U^* = f(p_k^*; c_l^*), \tag{4}$$

which expresses a joint dependence on the two sets of parameters. The variance in the result is then given by

$$[\delta U]^2 = [\delta U]_M^2 + [\delta U]_C^2, \tag{5}$$

where each of the terms on the right-hand side is given by Equation A.3, the first term arising from the analysis of experiment M and the second from experiment C.

The point of this discussion is that in the limit of a large number of measurements in experiment M (N large), knowledge of the $\{p_k^*\}$ becomes very exact and the first term in Equation (5) becomes small; however, repeated measurements in experiment M do not change the amount of information available in experiment C, and the values of the $\{p_k^*\}$ are contingent on the values of $\{c_\ell^*\}$. Hence, the value of the second term in Equation (5) does not change. While the underlying errors in both experiments are random, from the standpoint of the measurement (experiment M), we denote the first term in Equation (5) as a *random* error, since it can be made small by doing repeated measurements, whereas we denote the second term a *systematic* error, since it is unaffected by repeated measurements. ("Error" in the sense that we use it in Equation (5) is, of course, an estimate of the probability that the true result differs from the measured one; i.e., the true value should be between U-δU and U+δU with the same probability that a gaussian-distributed random variable lies within one standard deviation of the mean.)

It is useful to define a second type of systematic error. If in Equation (1) we defined our experiment as determining W_S and did the analysis accordingly, then the above discussion would apply without further comment. If, however, the experiment is defined as a measurement of W, then the experiment has a *bias* --the measured value must be corrected for flanking losses and thermal storage in order to obtain the correct U-value. Any errors in the corrections are clearly not random measurement errors in the sense of Equation (5), and it is useful to extend the category of systematic errors to encompass them. If the corrections are derived theoretically, then some estimate of the reliability of the calculation is a necessary part of a statement about systematic errors. If the dominant source of systematic error arises from a calculation, then it is clearly not possible to make a statistically precise error statement; however, if the estimate shows that the calculation is not a dominant error source, then theoretical estimation can be consistent with precise error estimates.

For these reasons, we define systematic errors to include both the effects of uncertainties in calibration of the experimental apparatus and uncertainties in biases inherent in the experiment.

ERROR SOURCES IN THE MOWITT

Electronic Noise

Most data in the MoWiTT are collected through a multiplexed digital voltmeter (DVM) with a 5 1/2-digit accuracy. On its most sensitive voltage setting, it has an accuracy on the order of 10 microvolts. Because most sensors have long cables, the dominant source of random measurement error is electronic pickup noise, which may be anywhere from a few to several thousand microvolts, depending on the quantity being measured, the measurement circuit impedance, the cable routes, and shielding.

Temperature Errors

Temperature measurements not requiring extreme accuracy (which includes most air temperature measurements) are made using an interchangeable, linearized thermistor composite, which is a small bead containing two thermistors of differing resistance that are connected together through a resistance network external to the bead. Electronic noise in these measurements accounts for a random temperature error always less than 0.03°C and usually much less. Self-heating corrections to the temperature readings are on the order of 0.06°C; however, since all thermistors of the same type are driven with the same current source, this correction cancels out when

temperature differences are measured. The dominant source of error for these measurements is the tolerance in the temperature specification, which is a systematic error on the order of 0.2°C.

Energy Flow Measurement Errors

The net energy flowing into each of the calorimeter chambers is derived from the equation

$$W = -(\ P_H + P_C + P_S\ ), \tag{6}$$

where P_H is the total electrical power added to the chamber, P_C is the power added by the liquid-to-air heat exchanger, and P_S is the power flowing into the chamber from the calorimeter walls.

All electrical power entering a calorimeter chamber is metered using specially designed wattmeters that make an analog multiplication of current and voltage waveforms and convert the product into a frequency-modulated pulse train. These pulses are counted and the accumulated count read by the computer. The result is that each pulse corresponds to an energy Q_0, and for the k^{th} wattmeter a reading of N pulses over a time τ yields a measured power of

$$P_{Hk} = Q_{0k}\frac{N}{\tau}, \tag{7}$$

where Q_{0k} denotes the value of Q_0, applicable to the particular wattmeter. (There are five wattmeters for each chamber, of which two are normally used during nighttime U-value measurements.) Periodic calibration of the wattmeters maintains the absolute accuracy of each wattmeter at the greater of 0.5% of the reading or 0.3 W. There is in addition an average reading error of $Q_{0k}/(\tau\sqrt{3})$ arising from the digital nature of the measurement. This error is not statistical in origin but does decrease with increased sampling time.

The power extracted by the fluid-to-air heat exchanger is determined from the flow rate and temperature change of the cooling fluid (P_C is defined as negative for heat extraction):

$$P_C = (\rho c_p) f[T_{in} - T_{out}], \tag{8}$$

where ρ is the fluid density, c_p the specific heat, f the volumetric flow rate, and T_{in} the inlet and T_{out} the outlet fluid temperatures. To prevent errors from heat conduction to or from fluid pipes, the temperature measurement sensors are located at the points where the fluid enters and leaves the calorimeter chamber. Flow is measured with a turbine flowmeter and normally varies by no more than 10% (usually much less). The cooling system is a constant-flow system, but slow variations in flow do occur due to the buildup of material in the fluid filters protecting the flowmeters. Temperatures are measured by two precision platinum RTDs. Noise in the latter measurements constitutes the only significant source of random error in the cooling system measurement; individual (5-second) temperature difference measurements have approximately a 0.03°C random error, which, through averaging of many readings, becomes around 2 mK for a 10-minute reading, the normal data-recording interval. This corresponds to 0.7 W random error for each data point. A U-value measurement is an average over many such points (typically ~300), implying a random error on the average of ~0.02 W. Periodic in-place calibration of the cooling power monitoring system maintains the total systematic error in the measurement at less than 0.6 W.

The power P_S flowing into the chamber from the insulated walls is measured by large-area heat flow sensors that cover approximately 90% of the interior calorimeter surface. These heat flow sensors were designed to have approximately 5% accuracy. They are chiefly important for daytime measurements; for the nighttime measurements used to derive U-values, the value of P_S is quite small (typically ~1 W), and uncertainties in the measurement of P_S are negligible.

Control System Short-Term Cycling

If one observes a high-resolution plot of the heater power, one finds short-term, apparently random, fluctuations in heater power that are much too large to be explained by the instrumental errors discussed above. These are caused by temporary excursions of the temperature control system that arise from the inherent time delays in the control system and the fact that the control system must apply a finite unit of power to correct a temperature undershoot. In fact, there is a reciprocal relationship between the accuracy with which the control sensor is maintained at the setpoint and the amount of power fluctuation. In general, the control algorithm is chosen to find the best compromise between close temperature control and minimum nighttime power fluctuations.

We assume the underlying temperature fluctuations causing these power fluctuations to be random. In that case, if over a given time interval the observed RMS fluctuation in the heater power is δP_S, the error in the average power measured over that same interval will be $\delta P_S/\sqrt{N}$, where N is the number of power measurements made over the measurement interval (and used to compute δP_S). A typical value for δP_S is 6 W for a 10-minute measurement interval, which corresponds to a 0.3 W random error in the long-term average used in the steady-state U-value measurement.

Flanking Heat Loss

As indicated in Equation (1) and Figure 2, the heat flow that is measured in the MoWiTT is the net heat flow through the portion of the calorimeter wall not covered by the large-area heat flow meters, which includes both the test sample and a portion of the mask and bridging walls. The detail of the sample wall interface is shown in Figure 3(a). To evaluate the heat flow through this complicated detail, a two-dimensional heat flow calculation was done using a finite-difference computer program (EE 1989). The resulting heat flow plot is shown in Figure 3(b). The calculation was repeated for a number of different sample thermal resistances and geometries to evaluate whether the heat flow pattern in the mask and bridge wall depends on the fenestration characteristics. No dependence on sample thermal resistance was found; there was a small dependence on sample thickness. The effective UA value of the mask and bridge wall (denoted M in Equation 1) was calculated from these simulations, neglecting the three-dimensional heat flow effects in the corners. The simulation was also used to model a measurement of the effective UA value in which the external surface of a frameless double-glazing sample was covered by a heated metal plate held at the same temperature as the calorimeter air. The calculated heat flow pattern indicated that the application of the heated plate made a negligible change in the heat flow pattern in the mask and bridge wall.

The calculated flanking loss correction was M=0.59 W/K. Measurements of the flanking loss using the heated plate yielded values of M=0.39 W/K and M=0.63 W/K, respectively, for chambers A and B. We take this to be reasonable agreement with the calculation and evaluate the systematic uncertainty in the correction from the RMS difference between the calculated value and the two measurements. We therefore take the flanking loss to be M=0.59±0.14 W/K. To compare this with the above estimates of errors in net heat flow, the estimated error for a temperature

difference of 20°C would correspond to a systematic heat flow error of 2.8 W, clearly a significant uncertainty.

Thermal Storage

While the use of large-area heat flow sensors eliminates the effect of thermal storage in the chamber walls, there is still some minimal thermal mass inside the metering boundary: the air in the chamber, the heat exchanger and other equipment, a plywood floor, and part of the heat flow meters themselves. We have measured the effective thermal mass during one of the periodic "closed-box" tests that are used to check the overall net heat balance. In a closed-box test, the sample area is sealed against air motion and covered with an additional set of heat flow meters to produce a redundant measurement of the net heat flow through the sample aperture. Exterior plywood sheets are also mounted externally to shield the sample aperture from solar radiation. During one such test, the chamber interior temperature was slowly ramped up and down at a rate that allowed the temperature control system to maintain good temperature regulation. The resultant change in apparent heat flow was fit to the measured value of dT/dt to obtain the value of C in Equation (1) for each chamber. The resulting values were C= 101±2 J/K for chamber A and C= 112±2 J/K for chamber B. Since normally for nighttime U-value testing the value of dT/dt for the chamber air is less than 2 X 10^{-5} K/s, this correction is on the order of 2 milliwatts and is completely negligible, unless control system problems cause an unusual chamber temperature variation.

Chamber Temperature Stratification

A more subtle thermal storage effect can arise from changes in temperature stratification of the air inside the test chamber. Since some effort is made to allow natural convection on the interior side of the window, some degree of thermal stratification is inevitable in the MoWiTT as well as in any laboratory hotbox. Natural convection at the window tends to generate thermal stratification, and the amount of airflow that would be necessary to completely eliminate it is generally incompatible with avoiding forced convection at the window interior surface. Of course, a considerably greater amount of thermal stratification is a normal part of a building environment.

If there is thermal stratification, then there can appear in Equation (1) additional terms of the form

$$-\left\{ C_{TOP} \frac{d[T_{TOP} - T_{AVE}]}{dt} - C_{BOT} \frac{d[T_{AVE} - T_{BOT}]}{dt} \right\}, \qquad (9)$$

which describe the flow of heat into storage at the top of the chamber and out of heat at the bottom. It is possible for the time derivatives of the two spatial temperature differences to be non-zero even if the spatial average temperature, T_{AVE}, is constant, and if the thermal mass is not symmetrically distributed vertically then (9) may be non-zero also.

It is possible for this effect to arise in the MoWiTT when the exterior air temperature is changing (which is almost always the case). Then the increased window net heat flow due to the larger temperature difference causes a more rapid natural convective flow at the window, which may increase temperature stratification. The importance of this effect is currently being evaluated.

Air Infiltration

Air infiltration rates are monitored in the MoWiTT by monitoring the concentration in each chamber of a tracer gas injected at a known rate. The infiltration rates are extremely low by normal

building standards. In order to obtain an accurate measurement of the concentration decrease of the injected tracer gas, it is necessary to measure over long intervals; consequently, only hourly average infiltration rate measurements for each calorimeter chamber are available.

Very low wind speeds (less than 5 mph) characterize the normal nighttime conditions in Reno under which long-term U-value measurements are made. We find that under these conditions the infiltration rate is essentially constant. The dominant sources of air infiltration appear to be characteristic of the calorimeter chambers rather than of the particular sample windows. Normally, well-sealed, non-operable windows have been tested, but in a few tests involving operable windows with a measurable leakage rate, we have not observed a measurable difference in the infiltration rate when the windows have been covered with plastic or had their operable joints taped.

There are two possible air infiltration paths in the MoWiTT calorimeter chambers. One is through the only moderately well-sealed ducts carrying power and signal cables to the equipment room. Some air leakage along this path is necessary to provide pressure equalization between the calorimeter chambers and the external environment when the ambient pressure changes due to the movement of weather fronts. Since the equipment room and the calorimeter chambers are nominally at the same temperature, the heat flow associated with this air infiltration path is small.

The second air infiltration path is directly to the outdoors through the mask wall or the window sample. Prior to the summer of 1990, this air infiltration was dominated by a leak between the mask wall and bridging wall. Measurements taken before and after this leak was sealed indicated that under conditions of low wind speed (mean wind speed on the order of 3 mph, characteristic of normal nighttime winter conditions) the infiltration rate decreased from 1.4 m^3/h to 0.2 m^3/h for chamber A and from 1.3 m^3/h to 0.7 m^3/h for chamber B. The infiltration rate decrease, 1.2 m^3/h for chamber A and 0.6 m^3/h for chamber B, can unequivocally be identified as infiltration to the outside; it is uncertain to which infiltration path the residual infiltration should be assigned.

From this we can calculate upper and lower limits to the infiltration heat flow correction to the measured net heat flow. If the apparent net heat flow W_I due to infiltration is (for either chamber A or B)

$$W_I = K_{\left\{\begin{matrix}A\\B\end{matrix}\right\}}\left[T_O - T_I\right], \tag{10}$$

then $0.33\ W/K \le K_A \le 0.39\ W/K$ and $0.17\ W/K \le K_B \le 0.36\ W/K$. This net heat flow must be subtracted from the measured net neat flow in Equation (1).

A SAMPLE U-VALUE CALCULATION

As an illustration of the above-described procedures, we present the derivation of the nighttime U-value from a series of measurements made on a non-operable, double-glazed window with a thermally improved aluminum frame. These measurements were made over the period March 13-23, 1990, using data taken between the hours of midnight and 6:00 a.m. PST (or sunrise, if that occurred earlier). Nighttime outdoor temperatures varied between -5 °C and 10°C during the measurement period. There was a control system malfunction the evening of March 16,

and, consequently, data from the night of March 17 were excluded. The results of the measurement are presented in Table 1.

Table 2 presents a detailed breakdown of the error sources for this set of measurements. As can be seen, the errors are predominantly systematic. We assume that both systematic and random errors from physically distinct sources are uncorrelated and hence can be combined according to the normal square-root-of-sum-of-squares procedure.

It can be seen that the overall systematic error (or uncertainty estimate) is about 9% and is primarily due to RTD calibration, flanking heat loss, and air infiltration. The RTD calibration errors applying to these measurements are larger than those discussed above because of the particular way the RTD calibration data was applied in this case; it is expected that an improved procedure for applying the calibration information will bring that error down to the level discussed in the text. Since the estimates of error for flanking heat loss and air infiltration are theoretical and approximate rather than statistical, the overall level of systematic error quoted should be taken as a rough estimate rather than a statistically precise statement. Continuing studies of both air infiltration and flanking loss are expected to enable us to reduce the systematic errors from those sources in the future. Random errors, here estimated to be less than 1%, are much smaller than systematic errors.

We note that Elmahdy (1992) in a companion paper reports an error level of around 7% for a hot box measurement of a sample of comparable thermal resistance, a value we take to be representative of a well-characterized and calibrated laboratory hot box. Thus, an accuracy comparable to that of a laboratory hot box is achievable with MoWiTT.

We believe that the circumstance that systematic errors are much larger than random measurement errors is not peculiar to MoWiTT measurements but probably applies to measurements with other thermal facilities. Unfortunately, in the common practice, if any errors are quoted at all, they tend to be statements of reproducibility, i.e., random errors. The much larger systematic errors are frequently not specified.

Interior and Exterior Film Coefficients

Interior and exterior surface heat transfer coefficients ("film" coefficients) are implicitly contained in the measured U-value. Because the MoWiTT measurements are conducted under realistic interior and exterior conditions, the question of whether there has been an appropriate simulation of the film coefficient in the measurement situation does not arise, as it does with laboratory measurements. The film coefficients are thus not a source of measurement uncertainty. However, in order to compare the measurements either with U-value calculations or with laboratory measurements, a knowledge of the film coefficients is needed, and the corresponding uncertainty enters the problem as a "theoretical uncertainty" for calculations or an "adjustment uncertainty" for comparing laboratory measurements. (This uncertainty does not arise, however, if one makes a direct, simultaneous measurement of two different window systems.)

The effective exterior film coefficient is measured in MoWiTT by means of a "film coefficient meter" consisting of a sheet of glass backed by a heated metal plate. Between the plate (which is held at a constant temperature) and the glass is a thin layer of material matched in thermal conductance to several small, commercially available heat flow sensors that measure the heat flow rate to the glass. The entire unit is insulated around the edges and behind the heated plate and is mounted on the MoWiTT wall between the two test chamber openings. The film coefficient meter is approximately one foot wide and is the same height as the test samples. Heat flow measurements

are made along the meter's vertical centerline. Infrared photographs have verified that there are no horizontal temperature gradients in the central part of the glass, where the film coefficient measurement is made.

The film coefficient meter measures the average combined film coefficient to be 10.3±1.6 W/m^2K over the period of the U-value measurement. A vertically mounted pyrgeometer also measured the effective radiant temperature seen by the window, so that the measured film coefficient can be separated into radiative and convective parts, if necessary.

A simultaneous measurement of single glazing in the other calorimeter chamber both provides a second measurement of the exterior film coefficient and permits us to determine the interior film coefficient. We find a value of 7.1±0.4 W/m^2K, which is slightly lower than the assumed ASHRAE value of 8.3 W/m^2K. It should be noted that use of this value for the interior film coefficient depends on the assumption that the interior conditions are the same in the two calorimeter chambers.

We also note that this approach shares with both laboratory measurements and computer calculations the assumption that the interior and exterior boundary conditions can be characterized by a uniform average film coefficient in place of the complicated convective and radiative conditions that they actually experience. This assumption appears to provide adequate agreement between theoretical calculations and measurements; the errors that it actually introduces are unknown.

CONCLUSIONS

MoWiTT measurements can be used to derive nighttime steady-state U-value measurements with an error level comparable to that of a laboratory hot box. Effective film coefficients can be specified sufficiently well to permit a comparison between measurements and theoretical calculations. This allows a test of U-value calculation algorithms that is independent of the question of whether laboratory simulation of weather conditions is accurate or representative. Comparison of MoWiTT measurements with both calculated and laboratory-measured U-values is expected to aid in the development of standard rating techniques. In addition, direct, simultaneous comparisons between windows are possible, and these should be independent of uncertainties in film coefficient.

In discussing measurement uncertainties, one must distinguish between random error sources, which become less significant with repeated measurements or longer measurement times, and systematic error sources, which do not. In MoWiTT measurements of steady-state U-values, the most significant uncertainties arise from systematic errors. A systematic enumeration of these error sources and estimates of the magnitudes of the uncertainties has been presented. It has been shown that measurement uncertainties may be as large as 10% for an R-2 window; however, additional calibrations or improvements either already completed or planned are expected to considerably reduce the magnitudes of systematic uncertainties, particularly for the case of high-performance windows. In contrast to random errors, systematic errors may be corrected by after-the-fact calibrations and, hence, the uncertainties reduced.

It is somewhat surprising that commercial hotbox facilities do not supply a similar analysis of their calibrations and systematic uncertainties as a matter of course. Publication of such

information would greatly aid in the comparison of window properties and the definition of standard rating techniques.

ACKNOWLEDGMENTS

The author is indebted to the members of the MoWiTT technical staff, Dennis DiBartolomeo, Mary Hinman, Guy Kelley, Steven Lambert, Jonathan Slack, Michael Streczyn, and Mehrangiz Yazdanian, whose diligence in running and maintaining the MoWiTT were vital to the success of this project. Special thanks are due to Mehrangiz Yazdanian for her help in determining the effects of air infiltration and to Yakov Zholudov for raising the question of stratification.

This work was supported by the Assistant Secretary for Conservation and Renewable Energy, Office of Building Technologies, Building Systems and Materials Division of the U.S. Department of Energy under Contract No. DE-AC03-76SF00098.

REFERENCES

Berman, S.M., and S.D. Silverstein. 1975. Energy conservation and window systems. In Efficient use of energy. New York: American Institute of Physics.

Elmahdy, A.H. 1991. Heat transmission and R-value of fenestration systems using IRC hot box: Procedure and uncertainty analysis. ASHRAE Transactions, 98(1).

EE, Ltd. 1989. FRAME, A finite-difference computer program to evaluate thermal performance of window systems. Waterloo, Ontario, Canada

Klems, J.H.; S. Selkowitz; and S. Horowitz. 1982. A mobile facility for measuring net energy Performance of windows and skylights. Proceedings of the CIB W67 Third International Symposium on Energy Conservation in the Built Environment. Dublin, Ireland: An Foras Forbartha.

von Mises, R. 1964. Mathematical theory of probability and statistics. New York: Academic Press.

Orear, J. 1958. Notes on statistics for physicists. Report No. UCRL-8417.Berkeley, California: Lawrence Berkeley Laboratory.

Press, W.H.; B.P. Flannery; S.A. Teukolsky; and W.T. Vetterling. 1986. Numerical recipes. New York: Cambridge University Press.

APPENDIX A
REVIEW OF THE STATISTICAL THEORY OF MEASUREMENT

Any experimental measurement consists of a set of quantities (x_i,y) $(i=1,..M)$ it is possible to measure, together with a theory that relates the measured quantities to the measurement apparatus and the physical variables one seeks to measure with it. Generally this theory can be expressed as a functional relationship among the measured quantities and a set of parameters, a_k $(k=1,...P)$:

where i takes all of the values 1...M, k takes all the values 1...P, and one of the measured quantities, denoted y, is computable from the others using the theory. The parameters a_k will generally include the values of the physical quantities being measured and may also include parameters characterizing the apparatus. For example, in calibrating a resistance temperature detector (RTD) known to be linear over a certain range, the measured quantities might be the temperature of a controlled bath, T_n, and a corresponding resistance, R_n. The theoretical equation $R = R_0 + A\,T$ would be used in conjunction with a set of measurements, $\{T_n, R_n\}$, to determine the parameters A and R_0. Thereafter, the parameters A and R_0 would be used together with the theoretical equation to determine the (resulting) *parameter* T from the measured quantity R.

In general a set of N measurements of (x_i,y) is used to determine a set of values a_k^* of the parameters. Because the measurements contain random measurement errors, these parameter values are not the (unknown) true values but only the most probable estimates based on the set of measurements $\{(x_i,y)_n$ $(i=1,...,M;$ $n=1,...,N)\}$. If N is large enough so that the problem is statistically over determined, then standard statistical techniques (Press et al. 1986) exist to determine both the values a_k^* and the error matrix, i.e., the variances of and correlations between the parameters. These techniques also include tests (such as the chi-squared test) to determine whether or not the theoretical equation is correct, provided that the probability distributions of the measured variables are known. However, we will assume (as is usually true for engineering applications) that the correct underlying theory of the experiment is known (although some parameters characterizing the experiment may need to be determined), that the random experimental errors have a Gaussian probability distribution, and that the magnitudes of the experimental errors can be inferred from the scatter of the experimental measurements around the theoretical curve. The experiment is said to have a number of statistical degrees of freedom $N_D = N - P$, where P is the number of parameters determined from the data.

The overall result of the experiment, which we here denote U*, is then computed from the estimated values of the parameters a_k^*:

This is, of course, only the most probable value of U rather than the true value. However, if the number of independent random error sources is very large, then the central limit theorem of statistics (von Mises 1964) states that for large N_D, U^* will be gaussian-distributed about the true value of U and the distribution will have a standard deviation given by (Orear 1958),

$$[\delta U]^2 = \sum_k \sum_j \frac{\partial f}{\partial a_k} \frac{\partial f}{\partial a_j} E_{kj}, \tag{A.3}$$

where E denotes the error matrix of the parameters and is given by

$$E_{kj} = \left\langle \left(a_k - a_k^* \right) \left(a_j - a_j^* \right) \right\rangle \tag{A.4}$$

in which the angle brackets denote a statistical average. The indicated differences in parameters inside the parentheses are, for example,

$$\delta a_k = a_k - a_k^*, \tag{A.5}$$

the deviations from the most probable values; the diagonal terms of E are thus the variances in the parameters, and the off-diagonal terms are the correlations. The derivative terms in Equation A.3 are to be evaluated at a_k^*.

We note that for parameters that are uncorrelated, Equation A.3 reduces to the normal formula for propagation of errors and that the usual phenomenon of domination by a few error sources takes place; i.e., for uncorrelated parameters for which dak is smaller than the largest error source, dal, by a significant amount (e.g., a factor of ten), the effect of dak on the value of dU is negligible.

TABLE 1
Sample Derivation of U-Value from Measured Quantities

Quantity	Source	Units				
		m^2	°C	W	$\frac{W}{K}$	$\frac{W}{m^2K}$
P_H	Wattmeters			182.6		
P_C	Cooling Power			-94.9		
P_s	Heat Flow Sensors			-1.1		
W	Equation (6)			-86.6		
$[T_O - T_I]$	Thermistors		-20.07			
$\frac{W}{[T_O - T_I]}$	Derived from above				4.14	
	Corrections					
M	Flanking Loss				0.59	
$C\frac{dT}{dt}$	Thermal Storage			<.002		
K_B	Air Infiltration				0.27	
$\frac{W_S}{[T_O - T_I]}$	Derived from above				3.28	
A_T	Chamber Construction	1.115				
U	Equation (2)					2.95

TABLE 2
Error Sources and Their Effect on Sample U-Value

Quantity	Error Source	Error Units	Random Error		Systematic Error	
			Magnitude	Equiv. $\frac{\delta U}{U}$ (%)	Magnitude	Equiv. $\frac{\delta U}{U}$ (%)
P_H	Wattmeter Calibration	W			0.9	1.0
	Short-term Control System Cycling	W	0.33	0.4		
P_C	(ρ c_p) Calibration	$10^6 \frac{J}{m^3}$			0.02	0.7
	RTD Measurement	mK	0.1	0.6	7.0	5.6
P_S	Heat Flow Sensors	W	<0.1	<0.2	<0.1	<0.2
A_T	Mask Wall Construction	m^2			<.005	<0.4
$[T_O - T_I]$	Thermistors	K	0.04	.01	0.2	1.0
M	Estimation of Flanking Loss	W/K			0.14	4.3
$C\frac{dT}{dt}$	Chamber Temperature Time-Variations	W			<.002	negl.
K_B	Uncertainty about Air Infiltration Path	W/K			0.19	5.8
TOTAL FROM ALL SOURCES				**0.7**		**9.3**

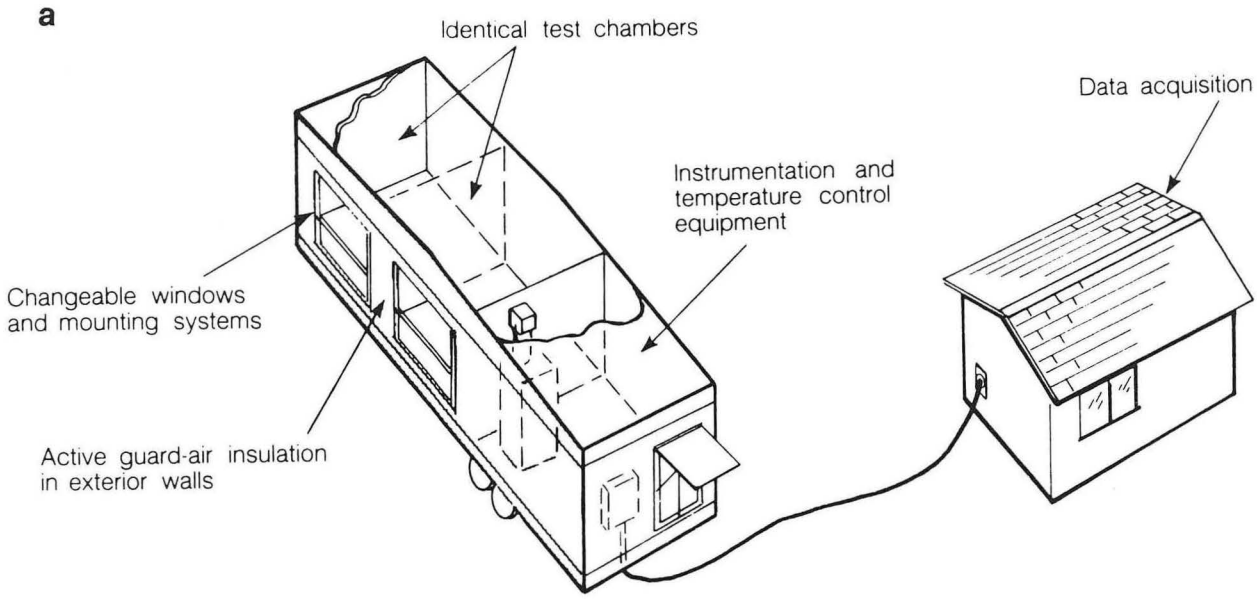

b

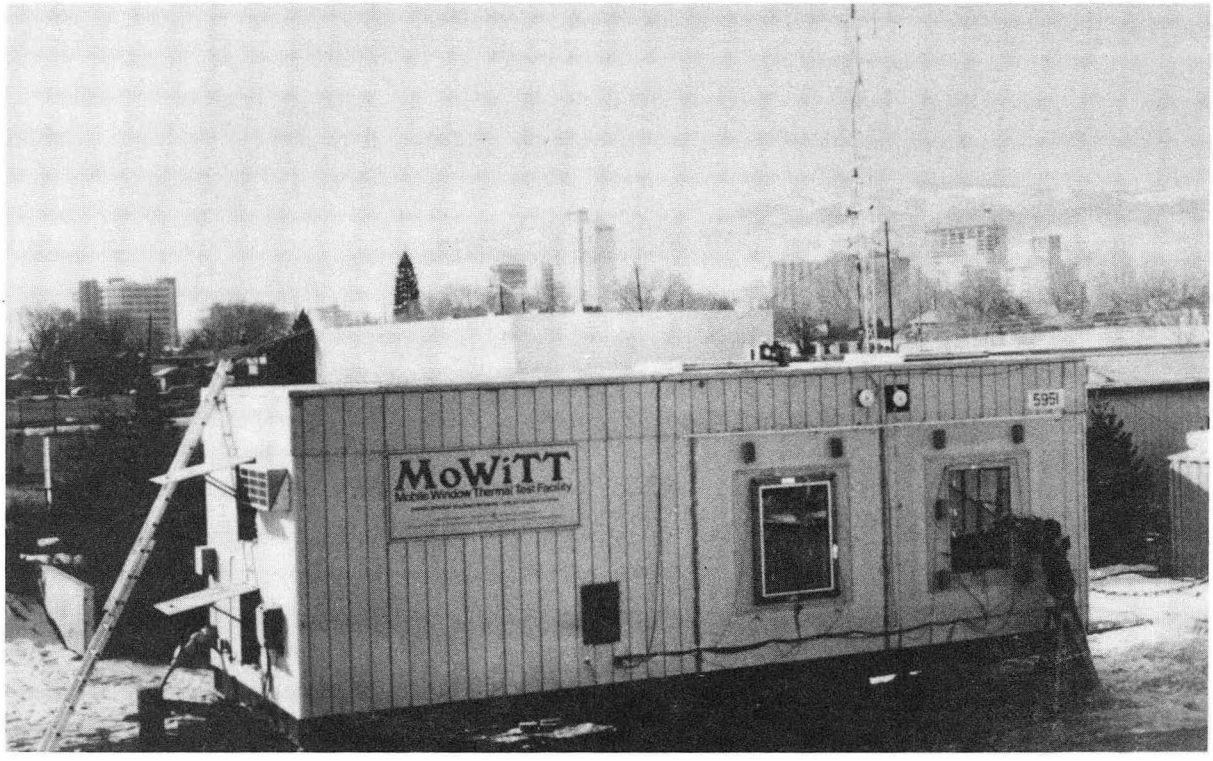

CBB 892-812B

Figure 1. (a) Schematic drawing of MoWiTT (Mobile Window Thermal Test) facility; (b) photograph of MoWiTT at the Reno, Nev., test site, winter, 1989.

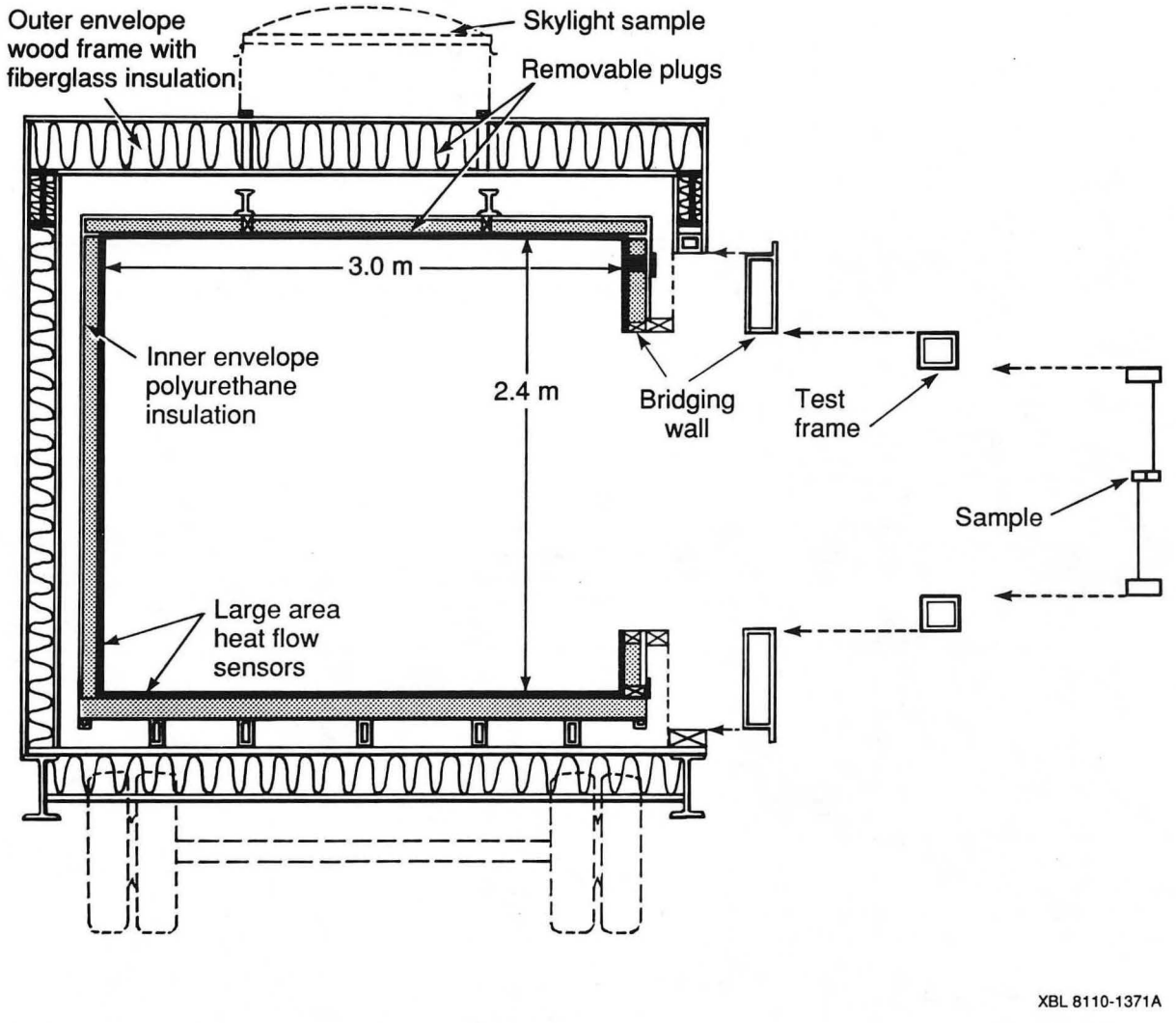

Figure 2. Cross section of a MoWiTT calorimeter chamber showing the mounting of a window sample in a test frame and bridging wall. As can be seen, the measurement aperture of the chamber (the area not covered by heat flow sensors) includes portions of the bridging wall and the test frame as well as the window sample.

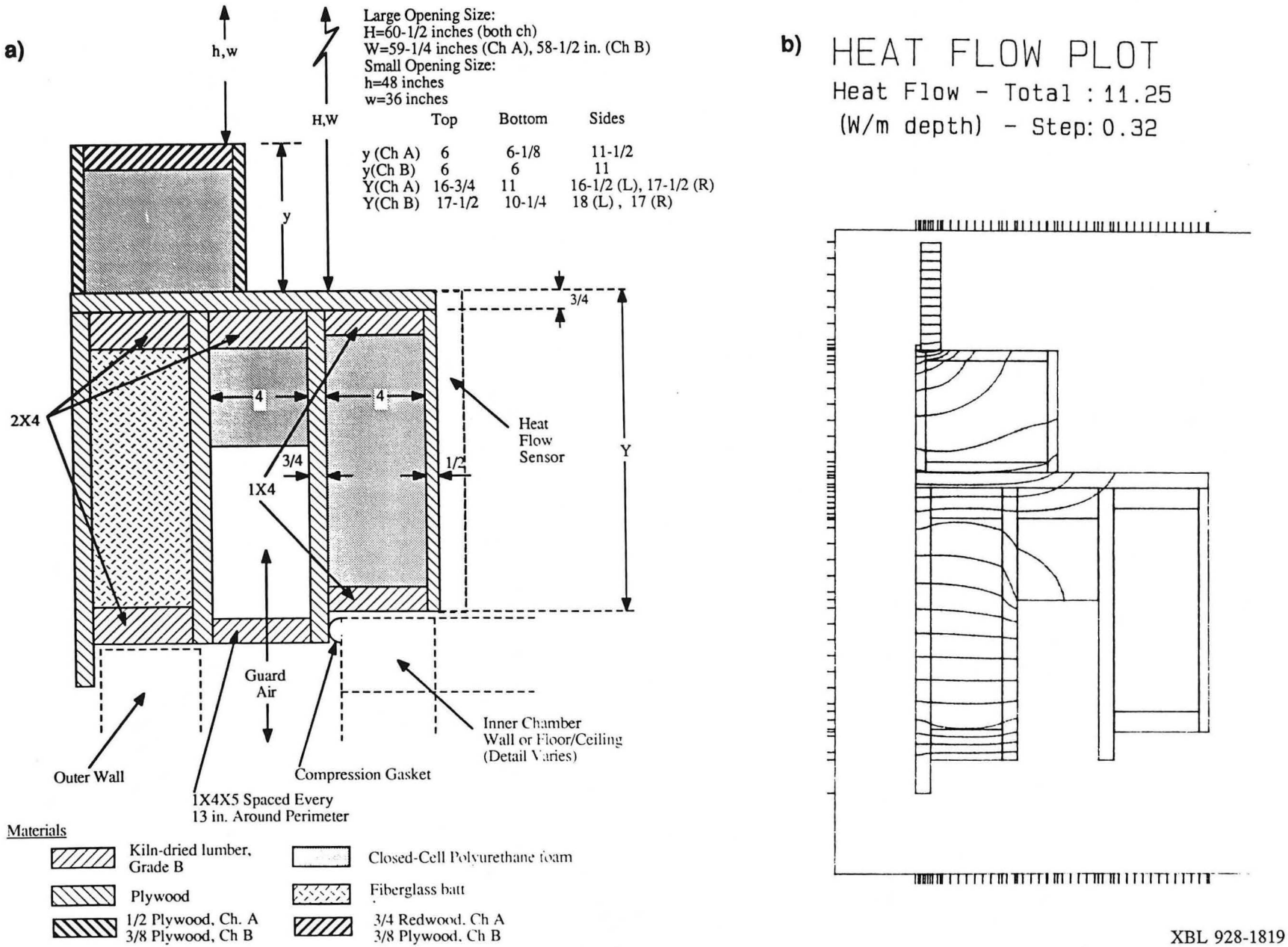

XBL 928-1819

Figure 3. (a) Detailed cross section of the bridging and mask wall; (b) plot of the calculated two-dimensional heat flow through the bridging and mask wall.

LAWRENCE BERKELEY LABORATORY
UNIVERSITY OF CALIFORNIA
TECHNICAL INFORMATION DEPARTMENT
BERKELEY, CALIFORNIA 94720